Fused-silica monolithic total-internal-reflection resonator

S. Schiller, I. I. Yu, M. M. Fejer, and R. L. Byer

Department of Applied Physics, Stanford University, Stanford, California 94305

Received October 23, 1991

We have characterized a miniature fused-silica monolithic optical ring resonator in which the Gaussian mode is confined by total internal reflection. Laser light is coupled into and out of the resonator by frustrating one of the total internal reflections by means of a prism. The resonator can be overcoupled and undercoupled by varying the resonator–prism distance. The minimum measured resonator linewidth was less than 3 MHz. This type of broadband, stable, low-loss resonator has applications in linear and nonlinear optics.

Broadband optical resonators that do not require thin-film-coated reflectors are of great practical importance, e.g., for tunable laser design. Achromatic cavities have been built by using discrete elements such as corner-cube retroreflectors,[1] prisms,[2] and variable outcouplers that use frustrated total internal reflection (FTIR).[3] However, for some applications monolithic resonators provide significant practical advantages such as mechanical stability and reduced optical losses caused by fewer interfaces encountered per round trip.[4] These two concepts may be incorporated in a single device, the monolithic total-internal-reflection resonator (MOTIRR).

Figure 1 shows a MOTIRR of refractive index n_1 that is appropriately shaped so as to sustain a closed ring path. If all angles of incidence θ within the resonator satisfy $\sin\theta > n_2/n_1$, where n_2 is the index of the surrounding medium, an optical wave is confined to the resonator. For example, a square ring requires $n_1/n_2 > 1.41$ and an equilateral triangular ring requires $n_1/n_2 > 2$. Coupling a wave into and out of the resonator is possible by using photon tunneling; if a medium of index $n_3 > n_1 \sin\theta$ is brought within a distance of the order of the wavelength from the resonator, total reflection is frustrated and a certain fraction of the wave will be coupled from the prism into the resonator or vice versa.

FTIR-coupled spherical MOTIRR's have recently been used as lasers[5] and have shown high finesse.[6] While modes of spherical resonators are described by Bessel functions, polygonal resonators with a finite number of reflections per round trip support Gaussian modes and have the advantage of facilitating mode matching between the input beam and the eigenmode. Microfabricated guided-wave MOTIRR semiconductor lasers have also been demonstrated.[7]

In an FTIR-coupled MOTIRR a wave is transmitted through the resonator by two tunneling processes. The amplitude of the circulating wave and hence of the output are resonantly enhanced when the wavelength-dependent round-trip phase shift leads to constructive interference between incoming and circulating waves.[8,9] Thus MOTIRR's are the optical analogs of microelectronic double-barrier heterostructure resonant tunneling devices.[10]

The frequency response of MOTIRR's can be derived as is done for standard Fabry–Perot resonators. Let t_j and r_j be the complex-field-transmission and reflection coefficients of an electromagnetic wave (vacuum wavelength λ_0) incident at an angle θ_j from medium j ($j = 1, 3$) upon a gap of thickness x and index $n_2 < n_j \sin\theta_j$ sandwiched between media 1 and 3. For a plane wave, the FTIR equations are[11]

$$|r_j|^2 = 1 - |t_1 t_3| = 1 - \frac{2\sin\gamma_1 \sin\gamma_3}{\cosh 2bx - \cos(\gamma_1 + \gamma_3)},$$

$$\arg(r_1) = \arctan\left(\frac{\sin\gamma_1 \sinh 2bx}{\cos\gamma_1 \cosh 2bx - \cos\gamma_3}\right), \quad (1)$$

where b is the inverse decay length of the evanescent wave,

$$b = \frac{2\pi}{\lambda_0}\sqrt{n_1^2 \sin^2\theta_1 - n_2^2}, \quad (2)$$

and γ_1 and γ_3 are the polarization-dependent phase shifts acquired by a wave that is totally internally reflected from the 1–2 and 3–2 interfaces, respectively,

$$\gamma_j = -2\arctan\left(\frac{m_j\sqrt{n_1^2 \sin^2\theta_1 - n_2^2}}{\sqrt{n_j^2 - n_1^2 \sin^2\theta_1}}\right), \quad (3)$$

where $m_j = 1$ for an s-polarized wave and $m_j = (n_j/n_2)^2$ for a p-polarized wave.

The amplitude of the total field E_r reflected from the ring cavity is given by

$$\frac{E_r}{E_0} = r_3 + \frac{t_1 t_3 \exp(i\phi)\exp(-\alpha)}{1 - r_1 \exp(i\phi)\exp(-\alpha)}, \quad (4)$$

where ϕ is the total phase shift acquired by the wave during one round trip and the factor $\exp(-\alpha)$ describes the round-trip field attenuation caused by optical losses. The reflected power is easily evaluated as[12]

$$\frac{P_r}{P_0} = \left|\frac{E_r}{E_0}\right| = 1 - \frac{c(x)}{1 + \left(\frac{2\mathcal{F}(x)}{\pi}\sin\left\{\frac{[\arg r_1(x) + \phi]}{2}\right\}\right)^2}. \quad (5)$$

0146-9592/92/050378-03$5.00/0

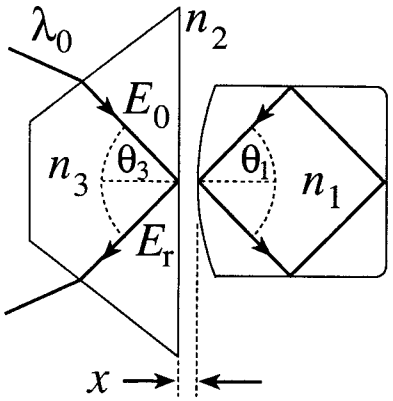

Fig. 1. Schematic of a monolithic total-internal-reflection resonator (MOTIRR). At each interface total reflection occurs, which can be controllably frustrated by a medium of index n_3 placed at a distance x of the order of the evanescent wave decay length $1/b$.

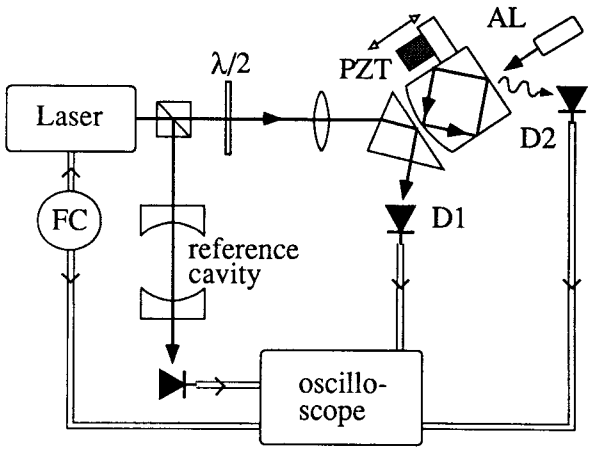

Fig. 2. Setup for measuring coupling and finesse of resonator modes as a function of gap distance x. FC, frequency control; AL, alignment laser. Resonances are detected by measuring the reflected power P_r (using D1) or the light scattered into detector D2 [signal $\sim c(x)$].

A MOTIRR thus exhibits the classic Fabry–Perot response, but with a gap- and polarization-dependent input-mirror reflectivity that leads to gap- and polarization-dependent resonance frequency $f_r(x)$, finesse $\mathcal{F}(x)$, and coupling $c(x)$, which are given by

$$2\pi f_r(x)/f_{\mathrm{FSR}} + \gamma_{\mathrm{tot}} = \phi_r(x) = 2N\pi - \arg r_1(x), \quad (6)$$

$$\mathcal{F}(x) = \frac{\pi\sqrt{\exp(-\alpha)\,|r(x)|}}{1 - \exp(-\alpha)\,|r(x)|}, \quad (7)$$

$$c(x) = \frac{[1 - \exp(-2\alpha)][1 - |r(x)|^2]}{[1 - \exp(-\alpha)\,|r(x)|]^2}. \quad (8)$$

Here f_{FSR} is the free spectral range, γ_{tot} is the sum of total-internal-reflection phase shifts caused by the remaining reflections, and N is an integer. For large gaps $x > 1/b$, and for small internal losses $\alpha \ll 1$, these quantities may be expanded as

$$\arg r_1(x) \simeq \gamma_1 + 2\exp(-2bx)\sin\gamma_1\cos\gamma_3,$$

$$\mathcal{F}(x) = \frac{\pi}{\alpha\{1 + \exp[-2b(x - x_m)]\}},$$

$$c(x) = \cosh^{-2}[b(x - x_m)]. \quad (9)$$

The gap distance $x_m = \ln(2\sin\gamma_1\sin\gamma_3/\alpha)/2b$ is the particular resonator-coupling prism distance at which the resonator is impedance matched. At resonance, as the gap x is increased, the resonator is first overcoupled ($c < 1$), then impedance matched [$|r(x_m)| = \exp(-\alpha)$], at which point the reflected power P_r vanishes, then undercoupled ($c < 1$ again). At the same time, the finesse monotonically increases to the asymptotic value π/α and the resonance frequency f_r decreases.

Our MOTIRR was fabricated with commercial, low-OH-content fused silica ($n_1 = 1.45$) and standard optical polishing techniques. Its dimensions 5 mm × 5 mm × 4 mm provide a nominally square ring path with a free spectral range $f_{\mathrm{FSR}} = 14.6$ GHz. For confinement of resonator modes, one of the faces was polished with a 13.5-mm radius of curvature, which yielded horizontal and vertical beam

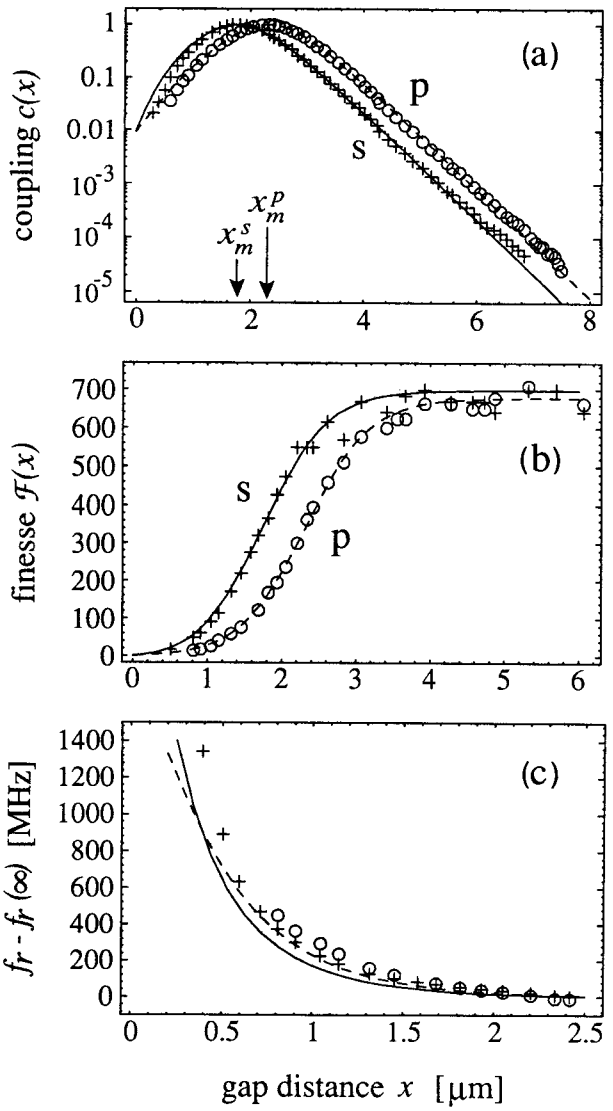

Fig. 3. Results of the scattered-light measurements for the TEM_{00} modes and comparison with theory. Crosses and solid curves show s polarization; circles and dashed curves show p polarization. (a) On-resonance couplings, normalized to the values at x_m. (b) Finesses. (c) Relative frequency shift. All curves are fitted according to Eqs. (6)–(8) by using the values for θ_1, α^s, and α^p given in the text and a common gap distance offset.

waists of 31 and 46 μm for the TEM_{00} mode at $\lambda_0 = 1.06$ μm.

The resonator was tested with a Nd:YAG single-frequency laser; the setup is shown in Fig. 2. Both the resonator and the coupling prism were mounted on mechanical stages that permitted control of all degrees of freedom. A visible laser was used to facilitate alignment with the probe laser and was used as an indicator of the gap size through observation of Newton's fringes. A piezoelectric actuator controls the prism–resonator gap; the resonator motion is measured by an inductive displacement transducer. A coupling prism of index $n_3 = 1.507$ was used. With our laser and a single mode-matching lens, we achieved 87% coupling into the fundamental mode. To study the resonator response as a function of frequency and gap, we polarized the laser at 45° and slowly thermally scanned over the *s*- and *p*-polarized resonances. A storage oscilloscope connected to a computer recorded the reflected or the scattered light power, as well as the response of a Fabry–Perot reference cavity. Figures 3(a)–3(c) show the data obtained by recording scatter from the circulating TEM_{00} modes, together with the theoretical fits. The losses and the evanescent wave decay length $1/b$ were determined from the asymptotic value of the finesses and the large-x decay [Eq. (9)] of the coupling, respectively. The fit yielded $b = (1.15 \pm 0.05)$ μm and losses of $\alpha^s = 0.0045$ and $\alpha^p = 0.0046$. The angle of incidence upon the coupling face was $\theta_1 = 44.7°$ by using Eq. (2), consistent with an independent measurement that showed the resonator to be slightly rectangular, with a 1.5% deviation from square. Under undercoupled conditions, the polarization shift $f_r^p - f_r^s$ between the *p* and *s* polarizations was measured to be 3.94 GHz, while Eq. (3) predicts a polarization shift of 3.90 GHz for this device.[13]

The finesse was found to be mode dependent owing to localized damage on the curved surface of the resonator. The TEM_{00} modes had a finesse of approximately 700, but a high-order mode exhibited a linewidth (FWHM) of 2.9 MHz, which corresponds to a finesse of 5100. The finesse was limited by the surface roughness and the contamination of the total-internal-reflection faces, which was evidenced by the large amount of scattered light visible and the appearance of thermal bistability at power levels of 10 mW. Finesses on the order of 10^5 should be possible by using ultrapure fused silica [bulk losses of 3 dB/km at 1.06 μm (Ref. 14)] and superpolishing techniques,[15] which yield a rms surface roughness of 0.05 nm, and scatter losses for four total reflections of less than 10^{-6} (Ref. 16).

This Letter demonstrates two applications of MOTIRR's: as ultrabroadband spectrum analyzers, and as submicrometer displacement sensors[17] through the gap dependence of the resonance frequency or of the power transfer function. MOTIRR's can serve as frequency references if operated with intensity-stabilized lasers and in a temperature-stable environment, especially if the environment is cryogenic. The potentially high finesse, broad spectral and temperature operating range, and adjustable impedance matching can also be exploited for nonlinear devices, e.g., doubly resonant or wideband second-harmonic generators and optical parametric oscillators, which can be used for generation of squeezed radiation.[18]

We thank M. Jain for his assistance and M. D. Levenson, A. Sizmann, and M. Karim for useful discussions. Support was provided by National Science Foundation grant PHY-89 13017.

References

1. E. R. Peck, J. Opt. Soc. Am. **53,** 253 (1962).
2. G. Marowsky and F. Zaraga, IEEE J. Quantum Electron. **QE-10,** 832 (1974).
3. I. N. Court and F. K. von Willisen, Appl. Opt. **3,** 719 (1964).
4. J. Y. Liou, C. J. Chen, and J. W. Chen, Appl. Opt. **19,** 653 (1980); T. J. Kane and R. L. Byer, Opt. Lett. **10,** 65 (1985); W. J. Kozlowsky, C. D. Nabors, and R. L. Byer, Opt. Lett. **12,** 1014 (1987).
5. T. Baer, Opt. Lett. **12,** 392 (1987).
6. V. B. Braginsky, M. L. Gorodetsky, and V. S. Ilchenko, Phys. Lett. A **137,** 393 (1989); S. Schiller and R. L. Byer, Opt. Lett. **16,** 1138 (1991).
7. S. Oku, M. Okayasu, and M. Ikeda, IEEE Photon. Technol. Lett. **3,** 588 (1991).
8. L. V. Iogansen, Sov. Phys. Tech. Phys. **11,** 1529 (1967).
9. J. R. Hull and M. K. Iles, J. Opt. Soc. Am. **70,** 17 (1980).
10. L. L. Chang, L. Esaki, and R. Tsu, Appl. Phys. Lett. **24,** 593 (1974).
11. M. Born and E. Wolf, *Principles of Optics* (Pergamon, New York, 1980); for a review of FTIR, see S. Zhu, A. W. Yu, D. Hawley, and R. Roy, Am. J. Phys. **54,** 601 (1986).
12. Using $\arg(r_1 r_3 / t_1 t_3) = \pi$.
13. Focal shifts of the near-critically internally reflected resonator mode contribute an additional 20 MHz for this device.
14. T. C. Rich and D. A. Pinnow, Appl. Phys. Lett. **20,** 264 (1972).
15. N. J. Brown, Ann. Rev. Mater. Sci. **16,** 371 (1986).
16. J. C. Stover, ed., *Scatter from Optical Components,* Proc. Soc. Photo-Opt. Instrum. Eng. **1165** (1989).
17. M. Allegrini, C. Ascoli, and A. Gozzini, Opt. Commun. **2,** 435 (1971); S. Schiller and R. Onofrio, Phys. Lett. A **154,** 221 (1991); M. F. Bocko, F. Bordoni, M. Karim, R. Onofrio, C. Presilla, S. Schiller, K. A. Stephenson, and N. Zhu, presented at Sixth M. Grossman Meeting, Kyoto, Japan, 1991.
18. A. Sizmann, R. J. Horowicz, G. Wagner, and G. Leuchs, Opt. Commun. **80,** 138 (1990).